Growth of bimolecular films of three-tailed amphiphiles

S. Kundu, A. Datta, and M. K. Sanyal
Surface Physics Division, Saha Institute of Nuclear Physics, Kolkata 700064, India

J. Daillant, D. Luzet, and C. Blot
LIONS, Service de Chimie Moléculaire, CEA Saclay, F-91191 Gif-sur-Yvette Cedex, France

B. Struth
European Synchrotron Radiation Facility, B.P. 220, F-38043 Grenoble Cedex, France
(Received 16 September 2005; revised manuscript received 28 March 2006; published 20 June 2006)

The three-tailed amphiphile ferric stearate molecule, which forms a bimolecular layer on water surface with molecules in the lower and upper layers in different conformations, has been studied to understand transfer and growth of bimolecular films on the surface of hydrophilic silicon substrates. This bimolecular film forms a two-dimensional lattice on water with a slightly distorted hexagonal lattice where both the in-plane and out-of-plane domain sizes are small. The film also showed larger microscopic rigidity compared to its macroscopic mechanical response. This asymmetric bimolecular layer was found to be preserved when the film is transferred on the substrates at different values of surface pressures ranging from 1 mN/m to near-collapse (55 mN/m). Both the upper and lower layers become denser and interfaces between these layers become sharper with increase in deposition pressure but the growths have different natures. The lower layer of transferred film is dense from 1 mN/m and, except for a steplike increase between 20 and 30 mN/m, changes slowly in density. The density of the upper molecular layer grows continuously with surface pressure.

DOI: 10.1103/PhysRevE.73.061602 PACS number(s): 68.03.Cd, 61.10.Kw, 68.18.−g

Organic monolayers formed at air-water interface by amphiphiles, molecules with a hydrophilic head and hydrophobic tail have been studied for more than 100 years [1]. Generally there is strong asymmetry of the molecules with respect to the air-water interface: the heads touch water and the tails stand out in air and the system is known as Langmuir monolayer [2]. However, amphiphiles may have multiple heads and/or tail, and their configuration at the air-water interface may lead to interfacial films with complex morphologies and interesting properties.

We have shown that molecules of a three-tailed amphiphilic salt, ferric stearate [FeSt, $(CH_3(CH_2)_{16}COO)_3Fe$], preformed and spread on water, form a film with anomalously high surface density, caused by the presence of pair of FeSt molecules in Y and inverted Y configuration of the tails about the Fe-bearing head groups, the tails in each pair being in an overall symmetric configuration about the head groups with one and one-half tails per head on the average [3]. We have also shown recently that this film is, in fact, a bimolecular film, where the molecules in the bottom layer are in the typical asymmetric configuration with the head touching water and all three tails on the same side of the head groups, i.e., up in the air, and the molecules in the upper layer form pairs in the Y and inverted Y configuration. The film, especially the upper molecular layer, was found also to grow in density with compression. This bimolecular film was found to reduce the surface tension of water by almost two orders of magnitude [4], and was quite different from usual Langmuir monolayer in its response to mechanical stress such as compression. We have shown that height fluctuations of water surface are drastically enhanced by the presence of this bimolecular film, giving rise to roughness primarily due to a capillary waves ~2.2 nm. This, in turns, gives rise to dramatic increase in the diffuse x-ray scattering intensity from this surface. However, Wilhelmy plate measuring surface tension cannot sense this effect [4]. It was also shown that horizontal transfer of the bimolecular film onto substrates from water surface does not make any remarkable changes either in the out-of-plane structure or the in-plane morphology.

For this complex bimolecular film with different molecular configurations in its two layers, the in-plane structure, in-plane and out-of-plane correlations, and in particular, the growth characteristics of the two layers are the important points to be understood. Growth is particularly interesting as the bottom layer of the film is dominated by hydrophilic interactions whereas the top layer has mostly hydrophobic forces acting on it [3] and tail-tail interactions stabilize this layer.

In this paper we have addressed these points regarding structure and growth of this bi-molecular film of FeSt molecules, through grazing incidence x-ray scattering studies of films on water surface and of films transferred onto Si(001) substrates using the horizontal deposition technique, which is a modification [4] of the inverted Langmuir-Schaefer method [5].

Preparation and purification process of FeSt has been described elsewhere [3,4]. 100 μL of 1.1 mg/mL solution of FeSt in chloroform was spread on Milli-Q water in a home-made Langmuir trough, at room temperature. The film was compressed at a rate ≈ 0.002 Å^2/molecule min and the surface pressure $\pi = \gamma_0 - \gamma$, where γ_0 and γ are the surface tensions of pure and film covered water, respectively, was measured with a paper Wilhelmy plate. X-ray scattering measurements were carried out using a 8.04 keV beam (wavelength 1.5421 Å) at the ID10B beamline of the European Synchrotron Radiation Facility. The same set up described in Ref. [4] was used to collect scattered intensity at

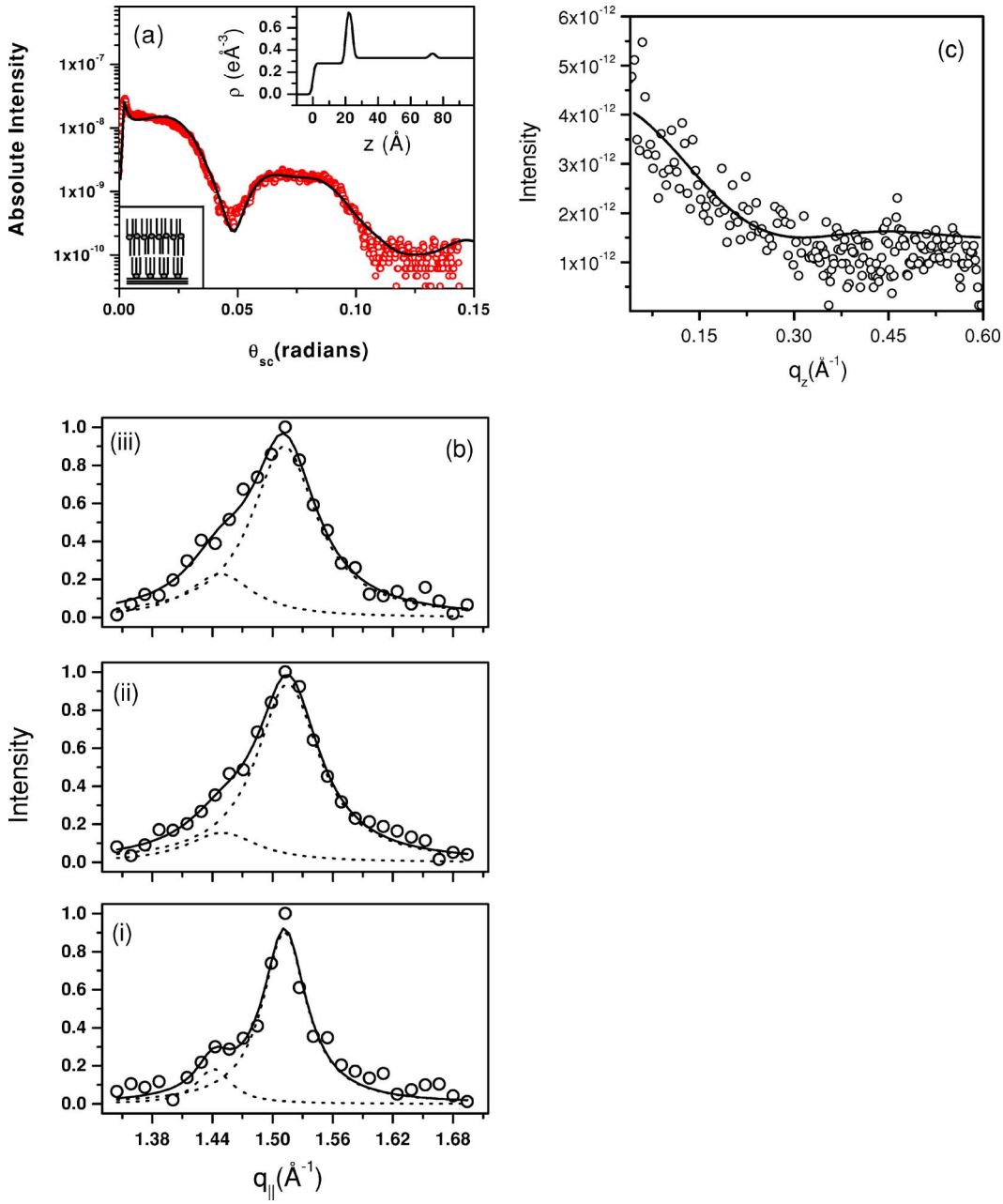

FIG. 1. (a) (Color online) Diffuse rod data (open circles) obtained from the FeSt film on water with low $q_{\|}$ value (ψ=0.2°). Solid line shows the best fit considering bimolecular configuration of FeSt molecules. Upper inset shows the electron density profile obtained from the fitting of the rod data and the lower inset shows the cartoon corresponding to bimolecular configuration of FeSt molecules on water surface. (b) Grazing incidence diffraction peaks of FeSt film on water for (i) π=1 mN/m, (ii) π=10 mN/m, and (iii) π=15 mN/m, respectively. Solid lines correspond to a two-peak Lorentzian functional fit with the two individual Lorentzian peaks shown by dotted lines. (c) Bragg rod profile of the FeSt film on water for π=1 mN/m (open circle) and solid line is the fit to the cylindrical model with one layer (≈20 Å thick).

grazing incidence but over a range of in-plane azimuthal angle (ψ), with respect to the specular plane, from 0° to Bragg angles corresponding to the in-plane lattice of the FeSt film on water surface. At each point the out-of-plane scattered intensity profile or rod as a function of the out-of-plane angle of scattering, θ_{sc} was collected by a position sensitive detector (PSD) while the in-plane scattering at that point was obtained by integrating over this rod. Data was collected for films at π=1 mN/m, 10 mN/m, and 15 mN/m [6].

Figure 1(a) depicts (open circles) a rod at ψ=0.2°, of the FeSt film at 10 mN/m surface pressure. The profile of the absolute intensity, i.e., the total out-of-plane scattered intensity with respect to the direct beam, as a function of θ_{sc}, the out-of-plane scattering angle measured from the horizontal, is presented. Model based on a bimolecular layer for FeSt molecules on water surface as shown in the lower inset of Fig. 1(a) [4] fits the data well. The curve obtained with this model is shown by the continuous line in Fig. 1(a) where the total scattering intensity follows Eq. (1) of Ref. [4] and the electron density profile (EDP) of the film, obtained from this

TABLE I. In-plane structural parameters of ferric stearate films on water.

Surface pressure π (mN/m)	Lattice type	Lattice parameters of in-plane unit cell **a** (Å)	**b** (Å)	Area/tail (Å^2)	Domain size (Å)
1	Distorted hexagonal (DH)	4.73	8.72	20.60	107 (Strong) and 150 (Weak)
10	DH	4.72	8.68	20.48	75 (Strong) and 60 (Weak)
15	DH	4.73	8.68	20.55	72 (Strong) and 71 (Weak)

fit, is shown in the upper inset of Fig. 1(a). The EDP shows that the model presented is somewhat idealized. In particular, the top monolayer with symmetrically configured molecules is not as tightly packed as the lower layer. The tails exposed to air are disordered and are free to tilt. This accounts for a lower density of this layer and also for the fact that the thickness of this layer is less than one-half of the hydrocarbon layer between heads. On the other hand, according to this model, the head/tail ratio in the bottom layer should be one-half of that in the top layer and this is actually borne out by the EDP, where the integrated electron density of the head group region in contact with water is much lower than that in the upper layer.

Figure 1(b) shows the in-plane Bragg peaks due to the lattice of the film at surface pressures of (i) 1 mN/m, (ii) 10 mN/m, and (iii) 15 mN/m. Two comparatively broad diffraction peaks could be observed, one main peak at 1.51 Å^{-1} and the other weak peak at 1.44 Å^{-1} for all π. Each diffraction data (open circles) is fitted by a two-peak Lorentzian function (solid line) with the two individual Lorentzian peaks shown separately (dotted lines). In absence of other peaks we have indexed the strong peak as $(11+1\bar{1})$ and the weak peak as (02) of a centered rectangular two-dimensional lattice [7] with the nonprimitive unit cell having lattice parameters **a** and **b** and untilted molecules at each lattice site. The centered rectangular lattice is equivalent to a symmetrically distorted hexagonal lattice. From Table I the in-plane structure is seen to be a distorted hexagonal lattice with the distortion parameter $\varepsilon=(\sqrt{3}-a/b)=0.1$ which is quite small. Such a slightly distorted hexagonal unit cell resembles the high temperature, high pressure rotator phase of behenic acid [8] than the phases observed on pure water for the same surface pressure and temperature [9]. The small variations in the lattice parameters are within the error bars. As there is no structural variation with increasing pressure the linear compression coefficients (inverse of the compressibility) of FeSt film cannot be obtained from GID. On the other hand from isotherm measure the linear compression coefficients are 34.5, 333.5, and 429 mN/m for 1, 10 and 15 mN/m surface pressures, respectively. Thus FeSt film on water shows large rigidity in the microscopic scale (as indicated by GID) whereas it is much less rigid in the macroscopic scale (as found from isotherms). Existence of near-invariant area per tail obtained in the GID measurement at very low average pressure of 1 mN/m indicate formation of disjointed clusters of FeSt molecular bilayers. These clusters join together as pressure increases but in-plane correlations remain quite small.

Figure 1(c) shows the profile of the rod collected by the PSD at the Bragg point, for films at $\pi=1$ mN/m (open circles). Profiles at 10 mN/m and 15 mN/m are found to be almost identical. These profiles have been fitted with the expression given for the cylindrical model [10] with n sections or layers and the best fit (shown as continuous line) is obtained with a one-layer model for the film, the thickness of the layer being 20 Å. Thus the crystalline correlation length along the normal to the water surface extends over one tail-layer of the bimolecular film of FeSt. The major source of this small correlation length along the bimolecular layer thickness may be a disorder in the packing of the upper layer. However, we cannot rule out the possibility of having two ordered but mutually uncorrelated molecular layers. Both in-plane and out-of-plane diffraction data rule out tilt of the molecules larger than 14° from the vertical.

To measure the π-A isotherm of the FeSt monolayer and to transfer the bimolecular film on to hydrophilic silicon (001) substrates, FeSt molecules were spread from a 0.7 mg/mL chloroform solution in a Langmuir trough (KSV 5000) on Milli-Q water at room temperature. A platinum Wilhelmy plate was used to measure the surface pressure of the FeSt monolayers. Monolayer was compressed with a speed of $\approx$0.49 Å^2/molecule min. A modified version of the inverse Langmuir-Schaefer method of horizontal deposition was employed to transfer the films. Depositions were done at 1 mN/m, 5 mN/m, 10 mN/m, 20 mN/m, 30 mN/m, 40 mN/m, and 55 mN/m surface pressure at room temperature with the substrate starting from below the films. Upward speed of the substrate holder was 0.5 mm/min for all transfers. X-ray specular reflectivity data were collected using a 18 kW rotating anode generator (Enraf Nonius, FR591).

It is seen from the isotherm presented in Fig. 4, in particular from the magnified region near zero pressure, that the pressure has started to rise roughly from 55 Å^2. From diffraction data, the area per tail is 20.6 Å^2, i.e., the area for three tails or the area per molecule in the monolayer should be $\approx$62 Å^2. The considerable reduction in the specific molecular area at zero pressure is consistent with the coexistance of monomolecular and bimolecular layers even at such low pressures. Beginning at this starting value of A the film has started to collapse nearly at 20 Å^2, that is area has decreased by a factor of 1/3. It implies that area per molecule A_m in monomolecular layer configuration is converted into area per molecule A_b in bimolecular layer configuration where total area occupied by one molecule is finally occupied by three molecules. The change from monomolecular to bimolecular layer configuration is shown by a cartoon in Fig. 2. This symmetric bimolecular configuration on top of asymmetric monomolecular configuration increases with increasing surface pressure.

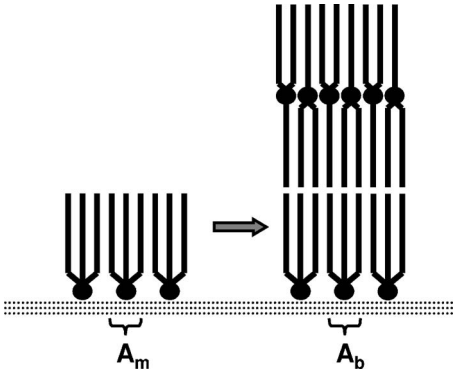

FIG. 2. Monomolecular to bimolecular layer formation with increasing surface pressure.

All x-ray reflectivity profiles and corresponding EDP's extracted from the fits using standard techniques [11] have been shown in Figs. 3(a) and 3(b) (color coded) in corresponding order. The films were taken to be on a layer of amorphous native SiO_2 on the Si(001) face. The bimolecular layer film is seen to be present from the lowest surface pressure to the highest. The thicknesses of the higher density and lower density regions of EDP's remain constant at about 8 Å and 20 Å, respectively, for all values of π and can correspondingly be assigned to the Fe-bearing head groups and the tails, consistent with the configuration shown in the lower inset of Fig. 1(a) at all deposition pressures. It is to be mentioned that a film transferred at the same deposition rate onto Si(001) by the vertical deposition method used in the LB technique at 30 mN/m, is a film of essentially a monolayer of asymmetrically configured molecules with a very low coverage of an upper layer of symmetrically configured molecules, indicating loss of the top layer during transfer. The EDP's clearly show the evolution of this configuration from a low density (coverage) film with large interface widths to a dense film with small interface widths achieving the bulk density of the tails ($\sim 0.27\ e/\text{Å}^3$) and the density of $0.48\ e/\text{Å}^3$ for headgroups. There is also an indication from the EDP's that the top and bottom layers do not evolve identically.

We have constructed a simple model for the bimolecular

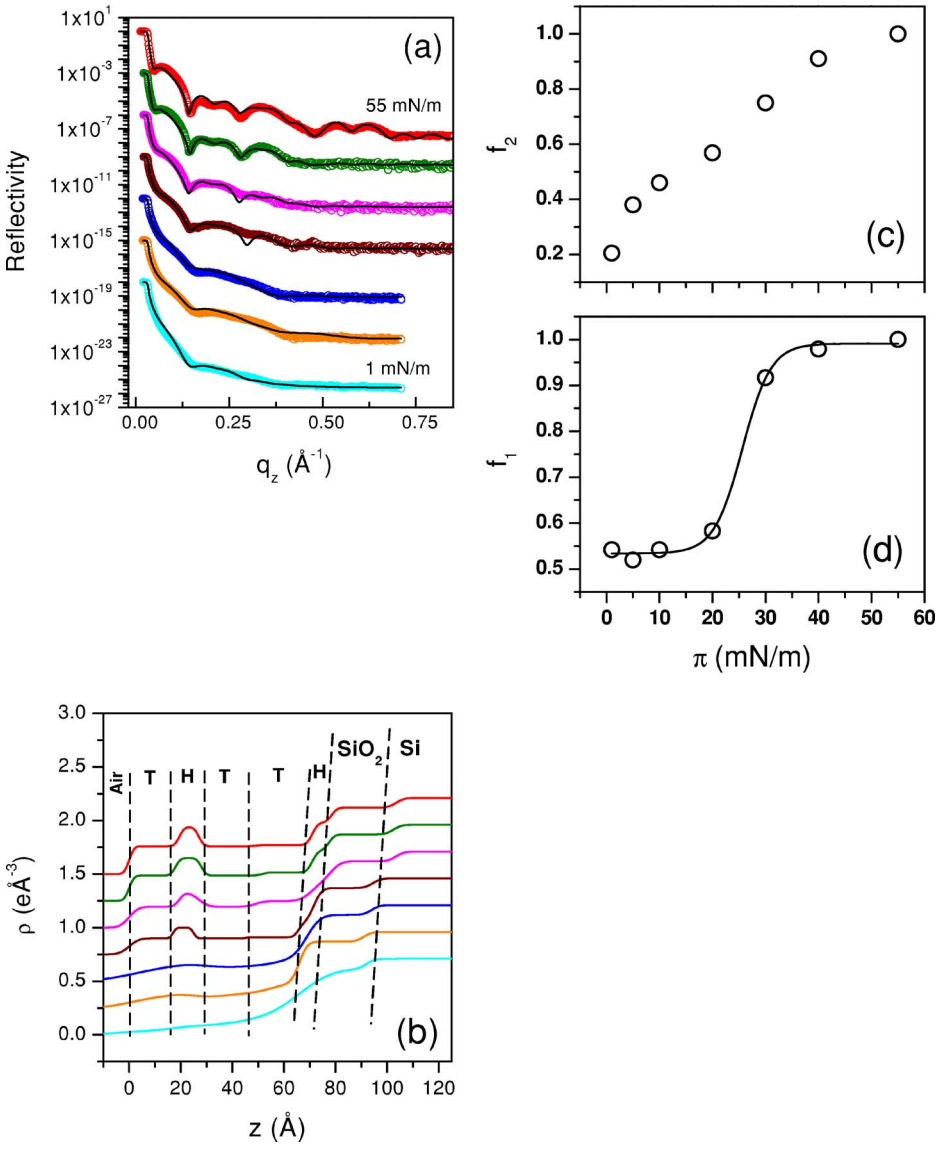

FIG. 3. (a) (Color online) X-ray reflectivity profiles (open circles) of the FeSt films deposited by horizontal deposition technique at surface pressures (π) of 1, 5, 10, 20, 30, 40, and 55 mN/m from bottom upwards, with the reflectivity profiles downshifted by multiplying in steps of 10^{-3} for clarity. Corresponding fits are shown by the solid lines. (b) (Color online) Electron density profiles (EDP's) extracted from the fit of reflectivity profiles given in (a) and color-coded accordingly. The Si/SiO_2, SiO_2/ film interfaces and head (H) and tail (T) regions in all films have been marked with dashed lines. For each profile air is at $z=0$. EDP's are upshifted by adding in steps of 0.25 with increasing deposition pressure for clarity. (c) f_2 vs π plot of the upper layer of FeSt film deposited by horizontal deposition technique where f_2 is the upper layer coverage and π is the surface pressure. (d) f_1 vs π plot of the lower layer of FeSt film deposited by horizontal deposition technique where f_1 is the lower layer coverage. Solid line is for the sigmoidal fit.

film from the extracted EDP's presented in Fig. 3(b). It is based on the assumption that the area per hydrocarbon chain is 20 Å^2. For the films transferred at the different values of π, we have varied the coverages of the bottom (f_1) and the top (f_2) layers as fit parameters and generated EDP's. It is observed that the model calculation and the best fit curves match at higher surface pressures while the model gives a very good estimate with all essential features at lower pressures. Both the upper and lower layer coverage depends upon the surface pressure. While the coverage of the upper layer (f_2) grows continuously [Fig. 3(c)] the lower layer behaves quite differently with pressure [Fig. 3(d)]. Instead of the nearly continuous change in coverage observed for the top layer, the bottom layer is quite dense ($f_1=0.54$) from the beginning and changes very little until $\pi=20$ mN/m, indicating the presence of the monolayer (with asymmetric configuration) as the precursor layer. Between 20 mN/m and 30 mN/m there is a sudden condensation of the bottom layer to $f_1=0.92$ coverage. This is about the same surface pressure for a transition to the solid phases of amphiphilic fatty acids [9]. The bottom layer coverage then slowly maximizes to 1.0 at 55 mN/m and practically merges with the top layer coverage, ending in a totally condensed film. Hence between 20 mN/m and 40 mN/m there is a large difference between f_1 and f_2 while between 40 mN/m and 50 mN/m this difference is negligible. This gives rise to the plateaulike region between 40 mN/m and 50 mN/m compared to the steeply rising region between 20 mN/m and 40 mN/m.

Now we can combine the information obtained from isotherm and x-ray reflectivity analysis. If we think at any pressure the increasing factor of bimolecular layer on top of the monomolecular layer is f_2 then at that pressure the area in the isotherm

$$A = A_m + A_b = (1 - f_2)A_m + f_2 A_b. \tag{1}$$

As $A_b \approx 1/3A_m$, hence

$$A = 3A_b - 2f_2 A_b = \mathcal{A}(\pi), \tag{2}$$

where $\mathcal{A}(\pi)$ is a function depends on the surface pressure. f_2 is obtained from the x-ray reflectivity fitting of the horizontally deposited films and if we plot $\mathcal{A}(\pi)$ considering the area where FeSt layer is in bimolecular configuration, i.e., $A_b \approx 20$ Å^2, we will obtain the curve as obtained from the π-A isotherm. The $\mathcal{A}(\pi)$ curve has nearly the same features with the π-A isotherm as shown in Fig. 4, implying monomolecular layer to bimolecular layer conversion with increasing surface pressure and with an initial combination of more monomolecular layer and less bimolecular domains. The formation of the symmetric structure at very low surface pressures underscores the importance of this molecular configuration in films of amphiphiles with multiple tails on water surface. Though the exact mechanism behind formation of such bilayers at even zero pressure is not understood. The above results also show the requirement of molecular information, obtained from microscopic methods such as x-ray scattering techniques, to understand the π-A isotherm of these films. As it is observed that the isotherm depends on the rate of compression, the time issues are approximately taken into account in the above analysis.

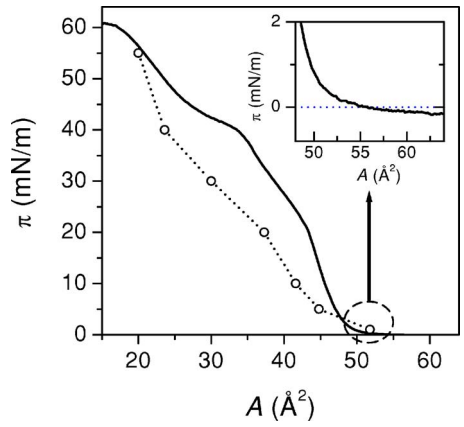

FIG. 4. (Color online) π-A isotherm (solid line) from Wilhelmy plate measurements and the function $\mathcal{A}(\pi)$ (open circle and dotted line) obtained from x-ray analysis. Inset, the low pressure region magnified, as indicated.

Here it is important to say that the paper Wilhelmy plate is not stable for surface pressure more than 20 mN/m and hence cannot measure above that value but platinum Wilhelmy plate can measure up to 60 mN/m. Thus for a particular state of the FeSt monolayer the surface pressure obtained from paper Wilhelmy plate, platinum Wilhelmy plate, and x-ray scattering are different. Similar situations have been noted for two-phase coexistence, such as for the liquid condensed (LC) and liquid expanded (LE) phases of pure fatty acid Langmuir monolayers, where the LC phase is dispersed as islands, stabilized by long-range dipolar forces, in the LE phase [12].

In conclusion we have shown that bimolecular layer of preformed ferric stearate on water surface can be transferred on a hydrophilic silicon substrate by a horizontal deposition technique and the mechanism of monomolecular to bimolecular layer formation with increasing surface pressure is understood combining the results obtained from x-ray reflectivity analysis and π-A isotherm. While the upper monomolecular layer of symmetric molecules grows continuously, the growth of lower monomolecular layer of asymmetric molecules is like conventional Langmuir monolayer—drastically different growth mechanism of two adjacent monomolecular layers is consistent with the fact that these layers are not structurally correlated.

[1] Lord Rayleigh, Philos. Mag. **48**, 321 (1899).
[2] G. L. Gaines, *Insoluble Monolayers at the Liquid-Gas Interface* (Interscience, New York, 1966); A. Ulman, *Introduction to Ultrathin Organic Films* (Academic, New York, 1991).
[3] A. Datta, M. K. Sanyal, A. Dhanabalan, and S. S. Major, J. Phys. Chem. B **101**, 9280 (1997).
[4] A. Datta, S. Kundu, M. K. Sanyal, J. Daillant, D. Luzet, C. Blot, and B. Struth, Phys. Rev. E **71**, 041604 (2005).
[5] T. Kato, N. Matsumoto, M. Kawano, N. Suzuki, T. Araki, and K. Iriyama, Thin Solid Films **242**, 223 (1994).
[6] J. Daillant and M. Alba, Rep. Prog. Phys. **63**, 1725 (2000).
[7] F. Leveiller, D. Jacquemain, L. Leiserowitz, K. Kjaer, and J. Als-Nielsen, J. Phys. Chem. **96**, 10381 (1992).
[8] C. Fradin, J. Daillant, A. Braslau, D. Luzet, M. Alba, and M. Goldmann, Eur. Phys. J. B **1**, 57 (1998).
[9] V. M. Kaganer, H. Möhwald, and P. Dutta, Rev. Mod. Phys. **71**, 779 (1999).
[10] D. Jacquemain, S. G. Wolf, F. Leveiller, M. Lahav, L. Leiserowitz, M. Deutsch, K. Kjaer, and J. Als-Nielsen, Colloq. Phys. **C7**, 29 (1989).
[11] L. G. Parratt, Phys. Rev. **95**, 359 (1954); J. K. Basu and M. K. Sanyal, Phys. Rep. **363**, 1 (2002); X.-L. Zhou and S.-H. Chen, Phys. Rep. **257**, 223 (1995).
[12] E. Ruckenstein, J. Colloid Interface Sci. **196**, 313 (1997).